Available online at www.sciencedirect.com
SCIENCE DIRECT
Catalysis Today 105 (2005) 350–356
CATALYSIS TODAY
www.elsevier.com/locate/cattod

Fischer–Tropsch synthesis using monolithic catalysts

Freek Kapteijn *, Ronald M. de Deugd [1], Jacob A. Moulijn

Reactor and Catalysis Engineering, DelftChemTech, Delft University of Technology, Julianalaan 136, NL-2628 BL Delft, The Netherlands

Available online 11 July 2005

Abstract

Square channel cordierite monoliths have been loaded with alumina washcoat layers of various thicknesses (20–110 μm) and loaded with rhenium and cobalt resulting in a 0.1 wt.% Re/17 wt.% Co/Al_2O_3 catalyst. These monolithic catalysts have been tested in the Fischer–Tropsch synthesis in a temperature window (180–225 °C) under synthesis gas compositions ranging from stoichiometrically excess carbon monoxide to excess hydrogen (H_2/CO = 1–3). The results include data on the activity and selectivity of $CoRe/Al_2O_3$ monolithic catalysts for FTS under these process conditions. Washcoat layers thicker than about 50 μm appear to lead to internal diffusion limitations. Thinner washcoat layers yield, depending on the conditions, to larger amounts of α-olefins than alkanes for chain lengths below 10 carbon atoms. ASF and non-ASF chain length distributions are obtained for thin washcoats, whereby the chain growth probability increases from 0.83 to 0.93. Under certain conditions the amounts of alkanes even increase with chain length. These experimental results with different diffusion lengths have been used to analyze the effects of secondary reactions on FTS selectivity.

Keywords: Fischer–Tropsch; Monolith; Cobalt catalyst; Olefin; Paraffin; Selectivity; Diffusion limitation; ASF (Anderson–Schulz–Flory) distribution

1. Introduction

In Fischer–Tropsch synthesis a simplified reaction model comprises the adsorption of CO, the formation of a surface intermediate monomer by reaction with hydrogen, and a chain growth of surface intermediates with this monomeric species (Fig. 1). Termination can proceed either by hydrogenation of the surface species yielding an *n*-alkane or by a reductive abstraction to a 1-alkene. A polymeric growth process can describe the product distribution. In Fischer–Tropsch the chain growth parameter α indicates the chance that a surface intermediate grows further, resulting in the so-called Anderson–Schulz–Flory (ASF) distribution.

Through readsorption the alkene can either be hydrogenated at the catalyst or be reinserted in the chain growth process. Diffusion limitations inside catalyst particles can strongly affect the final product distribution. Both secondary reactions and diffusion limitations may give rise to deviations from the ASF distribution.

Post et al. [1] clearly demonstrated the effect of particle size and pore radius on the Fischer–Tropsch activity of $CoZr/SiO_2$ catalysts. Particles in the size range as normally used in fixed bed reactors can cause serious diffusion limitations resulting in lower activities and apparent activation energies.

In recent literature the effect of secondary reactions of α-olefins is regarded as the most plausible explanation for deviations in ASF distribution [2]. Iglesia et al. attribute these effects solely to diffusion limitations [3], but the extent of readsorption and secondary reactions of olefins is determined by more aspects. Diffusion, solubility and physisorption are all influencing the chances of escape or readsorption of an olefin in a catalyst particle, all three favour the readsorption of olefins with a higher carbon number. Kuipers et al. [4] chose for studying the chain length dependence of the paraffin to olefin ratio as a more sensitive parameter for the interference of (transport) processes rather than the deviations from the ASF product distribution.

* Corresponding author. Tel.: +31 15 278 6725; fax: +31 15 278 5006.
E-mail address: f.kapteijn@tnw.tudelft.nl (F. Kapteijn).
[1] Present address: Shell Global Solutions International B.V., Badhuisweg 3, 1031 CM Amsterdam, The Netherlands.

0920-5861/$ – see front matter © 2005 Elsevier B.V. All rights reserved.
doi:10.1016/j.cattod.2005.06.063

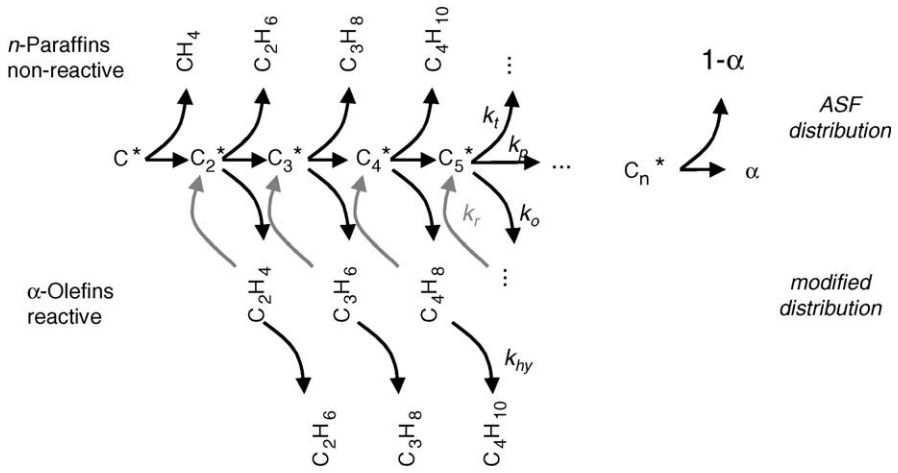

Fig. 1. Simplified reaction scheme of Fischer–Tropsch synthesis with chain propagation, termination by hydrogenation to paraffins and by reductive elimination to olefins and olefin readsorption.

Besides the effects of olefin readsorption, the intraparticle diffusion of carbon monoxide and hydrogen can give rise to effects on the selectivity of the Fischer–Tropsch synthesis. As the ratio between hydrogen and carbon monoxide concentration is important, differences in diffusivity between hydrogen and carbon monoxide also result in selectivity effects. Diffusion of hydrogen is faster than of carbon monoxide, leading to CO depletion and therefore an increase in the H_2/CO ratio towards the centre of the catalyst particle. The chain growth probability changes with this higher ratio, resulting in the production of more methane and other short chain molecules. Iglesia et al. [3] described this effect in their FTS selectivity model. In their model, olefin readsorption and CO depletion have an opposite effect on C_{5+} selectivity with varying characteristic diffusion length.

It is clear that diffusion limitations play a crucial role in the activity and selectivity of Fischer–Tropsch synthesis catalysts.

One of the large advantages of monolithic catalysts is the opportunity to apply thin catalyst layers with a tuneable thickness in a fixed body in a large-scale reactor with very low pressure drop [5,6]. Thin catalyst layers may eliminate effects of diffusion limitations. The tuneability of the layer thickness allows designing the monolithic catalyst with optimal activity and selectivity [7].

Only one other group reported on the application of monolithic structures in FTS [8–10]. The major conclusion from their work is that catalyst layers below 50 μm should be free of diffusion limitations, apparent from the highest activity and selectivity to C_{5+} products. Also the propene/propane ratio decreased. Only limited data are given in this study. Recently, monolith structures were investigated for a catalytic membrane configuration [11].

Here we report an extensive and systematic study of variation of the catalyst layer thickness on monoliths from 20 to 100 μm as a function of temperature and feed composition in order to experimentally determine the effects of internal mass transfer limitations on catalyst activity and selectivity. It is aimed for to arrive at guidelines for design of monolithic catalysts for Fischer–Tropsch synthesis.

2. Experimental

2.1. Monolith catalyst preparation

The experiments were performed with $CoRe/Al_2O_3$ on cordierite monoliths with different catalyst layer thicknesses. The choice for this rhenium promoted cobalt on alumina catalyst was made based on the work of Hilmen et al. [10]. The monolithic catalysts used in this study were prepared by washcoating γ-alumina on bare cordierite monoliths (Corning Inc.) with a cross section of 1 cm, lengths between 10 and 25 cm and a cell density of 200 channels per square inch (cpsi). Different coating thicknesses were achieved by repeating the coating process several times. In between two coatings the monoliths were dried in air for at least 12 h at ambient conditions and calcined at 450 °C. The washcoating procedure is described in detail by Nijhuis et al. [12].

The active phase has been applied by homogeneous deposition precipitation at 70 °C from an aqueous solution of cobalt nitrate, rhenium oxide and urea. As the urea decomposition is a slow process the cobalt hydroxide is deposited uniformly over the thickness of the washcoat [12]. The amount of cobalt nitrate in the solution is enough to reach the desired Co loading, 17 wt.%, on the alumina. As rhenium is not precipitated its amount will be lower than the targeted 1 wt.%. The role of rhenium is not well established, but it is thought to act as a structural promoter maintaining the dispersion of Co [13], and to play a role in the hydrogen dissociation for the reduction and in the reaction.

The catalyst was calcined in static air at 350 °C for 16 h decomposing the cobalt hydroxide to cobalt oxide. Before testing the catalyst is reduced in pure hydrogen at 350 °C for 2 h.

2.2. Characterization

The cobalt and rhenium loadings determined using XRF were 17 and 0.1 wt.%, respectively. The cobalt dispersion of crushed samples determined by H_2 chemisorption after reduction at 350 °C for 2 h amounted to 2–3%, so low relative to the postulated optimum of 10–12% [13]. This could be due to the applied reduction conditions. The TPR profiles correspond well with that of Arnoldy and Moulijn [14] and only Co_3O_4 is reduced, corresponding to about half the Co present. If the reduction is incomplete this translates into a low dispersion. The BET surface of the catalyst was 140 m^2/g, the porosity 31% and average pore diameter 7 nm, all determined by N_2 adsorption. These values exclusively reflect the properties of the Al_2O_3 washcoat.

SEM analysis revealed flat wascoat layers on the cordierite monolith channels with rounded corners where the layer is thicker. In the corners, cracks occur, especially for thicker washcoat layers (Fig. 2). Hence an unequivocal washcoat thickness could not be established. An average thickness has therefore been calculated using the geometric surface area of the cordierite support and the loading of the washcoat, accounting for density and porosity of the washcoat. The calculated layer thicknesses on the various monoliths range from 20 to 110 μm.

2.3. Set-up

The monoliths have been tested in a dedicated set-up for Fischer–Tropsch synthesis suited for testing monoliths [15]. The feed stream is mixed from high-pressure carbon monoxide, hydrogen and argon (internal standard) supply using separate mass flow controllers ensuring a fixed feed composition. The mixed synthesis gas is distributed to the reactors using individual mass flow controllers. The reactor effluent is lead through a gas–liquid separator operating at 175 °C to remove waxy liquid products. The gaseous stream is sent to a Chrompack GC (CP9001) equipped with a CP-Sil5 column and a FID detector to detect C_{5+} and a Molsieve 5 Å and Porabond column coupled to a TCD detector for detection of CO, Ar, and methane. This GC configuration allows analyzing a Fischer–Tropsch synthesis reactor effluent quantitatively up to C_{20} within 45 min.

2.4. Operating conditions

The monoliths have been tested in a window of temperatures (180–230 °C) and feed compositions (H_2/CO ratio = 1–3) at a total pressure of 15 bar and a fixed space velocity of 0.13 mol synthesis gas $kg_{cat}^{-1}\,s^{-1}$, including 4–6 mol% argon as internal standard. The inlet flow rate of synthesis gas was adapted to compensate for different weights of catalyst in the various experiments. The total mass of the $CoRe/Al_2O_3$ catalyst excluding the cordierite varied between 1.77 g for the monolith sample with a layer thickness of 20 μm to 6.76 g for the sample with a 110 μm thick layer.

The various experimental conditions have been applied in the same experimental run for each catalyst sample in a fixed order. First, the monolithic catalyst is stabilized under stoichiometric feed composition for at least 36 h before testing the catalyst with the same composition of the feed. After 12–15 h of isothermal operation the temperature is raised 10 K. After the final temperature the reactor is cooled down to the reference temperature, 210 °C, to check for activity changes. Subsequently, the experimental run is continued with a stoichiometric excess of hydrogen concentration in the feed using a similar temperature program. As a reference, after the temperature program the catalyst is tested again at the reference temperature with both the excess hydrogen feed and the stoichiometric feed. Finally, the same procedure is repeated with an excess carbon monoxide feed. This order of feed compositions is chosen to minimize effects of deactivation that may occur using excess carbon monoxide feed. Typically, a complete experimental run lasts for 250–300 h. Deactivation is

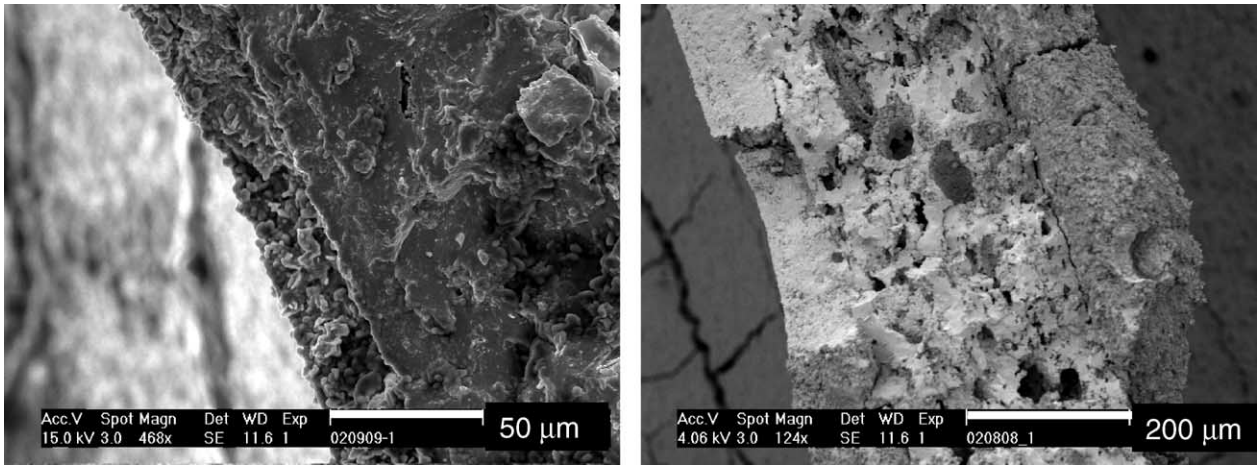

Fig. 2. SEM pictures of wall cross-sections (in the middle) of washcoated monoliths. *Left*: 30 μm (average) thickness sample and *right*: 110 μm thickness. Note the different magnification. The corner rounding and cracks are clearly visible in the latter sample.

typically limited to a few percent after the operation periods under stoichiometric and excess hydrogen conditions (about 200 h). In the excess carbon monoxide part of the experimental runs (the last about 100 h) the activity loss can increase to 20% of the initial activity under excess carbon monoxide after operation at 230 °C.

The catalyst activity has been defined as mol CO converted per kilogram catalyst (washcoat) per second, and hence represents an average over the reactor. The selectivities of the various reaction products were calculated on the basis of the molar fraction of that hydrocarbon in the hydrocarbon mixture.

3. Results

Fig. 3 shows a representative example of the activity of the monolithic catalyst with a washcoat layer of 30 μm for the three different feed compositions in the temperature window between 180 and 230 °C. An excess carbon monoxide leads to the lowest activity at higher temperatures. At lower temperatures, the activity in the excess carbon monoxide situation is comparable to that of the two other feed mixtures. Over the entire temperature range, the highest activity is reached with excess hydrogen concentration (H_2/CO = 3), but becomes less at higher temperatures. The CO conversion level in the test ranges from around 7% in the lower part of the temperature window to 50% and higher for temperatures of 220 and 225 °C with stoichiometric and excess hydrogen feed composition. In case of excess hydrogen and high conversion levels, the composition in the last part of the reactor may deviate from the inlet composition, as the H_2/CO consumption ratio is different from the feed ratio. In excess carbon monoxide, the maximum conversion is limited to only 20%, but it is emphasized that the molar flowrate of CO is also higher, since the space time of the syngas was kept constant.

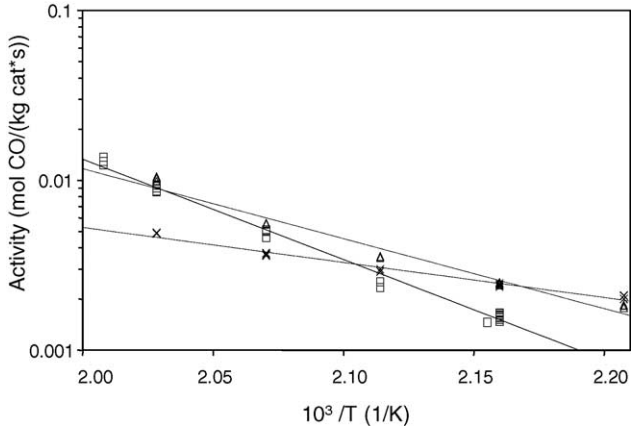

Fig. 3. Arrhenius plot of monolithic catalyst activity with 30 μm washcoat for three different feed compositions: (□) H_2/CO = 2, (△) H_2/CO = 3 and (×) H_2/CO = 1.

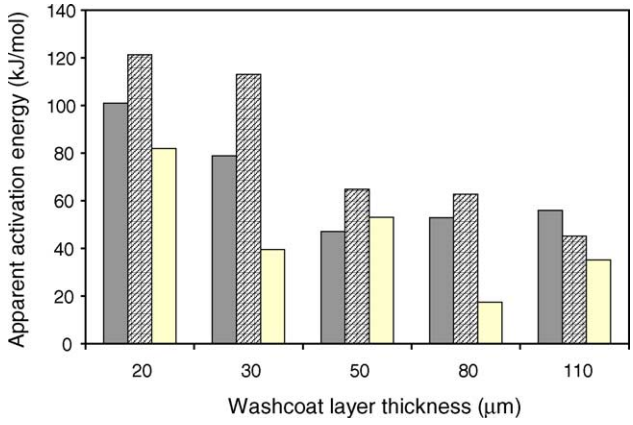

Fig. 4. Apparent activation energy of monolithic catalysts with different washcoat layers between 20 and 110 μm at feed composition H_2/CO = 3 (grey), 2 (hatched) and 1 (light).

The activation energies for the different washcoat thicknesses and the three feed compositions is presented in Fig. 4. A stoichiometric feed leads to the highest activation energy of ∼115 kJ/mol, comparable to literature [9], while excess CO leads to the lowest, ∼40 kJ/mol. Above layer thicknesses of ∼30 μm the observed activation energies clearly decrease, which may be attributed to interference of diffusional limitations.

The tests with monoliths of different washcoat thicknesses show similar activities, apparently the consumption of CO is only slightly affected (Fig. 5). In general the selectivity to methane increases with layer thickness (Fig. 5), strongly with temperature and with increasing hydrogen content (not shown). The methane selectivity for 110 μm deviates from the trend in layer thickness, in that it corresponds more to results with thinner layers.

Major FTS products of the monolithic catalysts are straight chain α-olefins and paraffins. A representative distribution in the C_6–C_{15} range for a catalyst with 30 μm

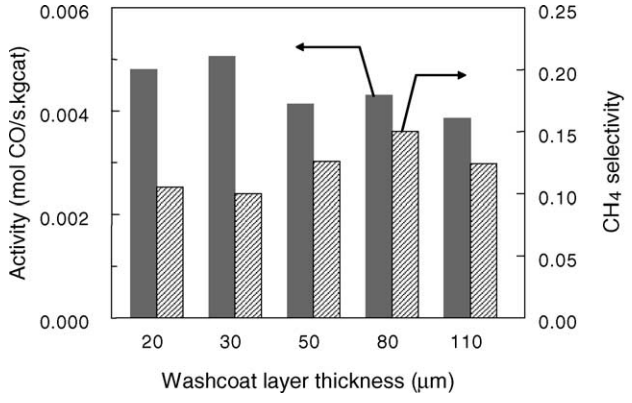

Fig. 5. Total activity in mol CO/(kg cat s) (*left*, dark bars) and methane selectivity (*right*, hatched bars) of monolithic catalysts with different washcoat layer thickness between 20 and 110 μm at 210 °C and stoichiometric feed composition (H_2/CO = 2).

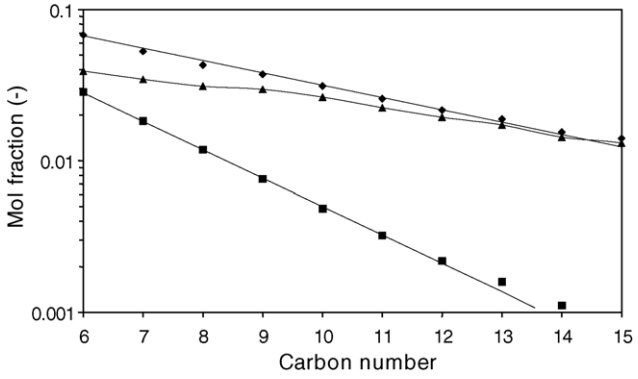

Fig. 6. Product distribution of monolithic catalyst with 30 μm washcoat layer at 210 °C and stoichiometric feed composition (H_2/CO = 2): (◆) total, (▲) paraffin and (■) olefin.

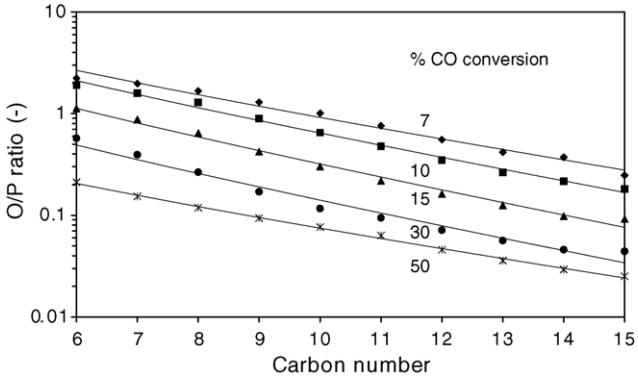

Fig. 8. Olefin to paraffin ratios of monolithic catalyst with 20 μm washcoat layer at different temperatures (180–220 °C) in log-normal plot (H_2/CO = 2): (◆) 180 °C, (■) 190 °C, (▲) 200 °C, (●) 210 °C and (*) 220 °C. Values of the CO conversion levels (%) at the different temperatures are included.

washcoat layer at 210 °C and a stoichiometric feed is given in Fig. 6. The *n*-alkanes are produced in excess over the 1-alkenes for C_5 and longer chain molecules under these conditions. The chain propagation parameter α in the ASF model for the sum of the *n*-alkane and 1-alkene products amounts to 0.84 over this range. Higher temperatures yield lower α-values.

Lower temperatures and decreasing H_2/CO ratios change this behaviour (Fig. 7). More 1-alkenes than *n*-alkanes are produced below C_{10} at 190 °C and H_2/CO = 1. The amounts of *n*-alkanes even increase over C_6–C_{15} product range, suggesting an α-value >1. The 1-alkenes follow the ASF-distribution in this range yielding an α-value of 0.77. For the total products this results in a changing slope of the ASF-plot, yielding an α-value of 0.83 up to C_{10} and of 0.93 above C_{10}.

The olefin to paraffin (O/P) ratio is a function of the temperature, feed H_2/CO ratio and washcoat thickness. The log-normal plots of the O/P ratio form more or less straight lines. With increasing temperature the O/P ratio decreases by a fairly constant factor over the whole C_5–C_{15} range (Fig. 8). Simultaneously the CO conversion levels, included in the figure, increase with temperature.

The decreasing feed H_2/CO ratio increases the O/P ratio considerably as depicted for the 30 μm washcoat monolith at 210 °C (Fig. 9). The hydrogen concentration appears a strong factor determining the O/P ratio. By introducing more hydrogen, the paraffin formation is strongly increased at the expense of the olefin content, but also the CO conversion increases. Under excess carbon monoxide conditions the olefin content is even higher than the paraffin content up to C_8 at this temperature. Off-line analyzed gas samples collected in gas bags shows that this trend extends down to C_3. Since the syngas molar flow is kept constant in these experiments the CO flowrate decreases with increasing H_2/CO ratio, and the total amount of CO converted per unit time increases only with 50% and not by a factor of 3 as the conversion would suggest.

With increasing washcoat thickness the O/P ratio decreases up to a factor of 6, shown in Fig. 10 for 210 °C and stoichiometric feed composition, while the CO conversion only decreases by 20% (Fig. 5).

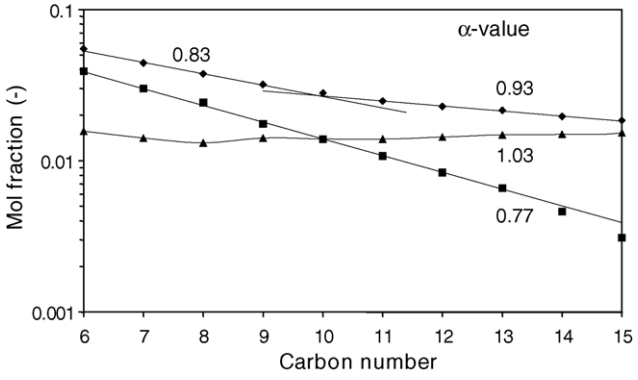

Fig. 7. Product distribution of monolithic catalyst with 30 μm washcoat layer at 190 °C and excess carbon monoxide feed composition (H_2/CO = 1) in log-normal plot: (◆) total, (▲) paraffin and (■) olefin.

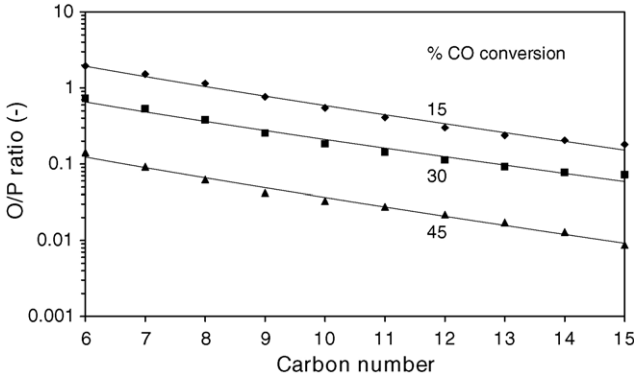

Fig. 9. Olefin to paraffin ratios of monolithic catalyst with 30 μm washcoat layer at 210 °C and different feed compositions (H_2/CO = 1–3) in log-normal plot: (◆) H_2/CO = 1, (■) H_2/CO = 2 and (▲) H_2/CO = 3. Values of the CO conversion levels (%) at the different compositions are included.

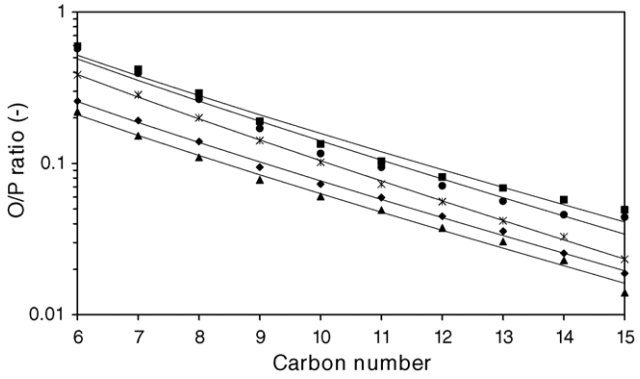

Fig. 10. Olefin to paraffin ratio of monolithic catalysts with different washcoat layers between 20 and 110 μm at 210 °C and stoichiometric feed composition (H_2/CO = 2) in log-normal plot: (●) 20 μm, (■) 30 μm, (*) 50 μm, (▲) 80 μm and (◆) 110 μm.

In most cases the linear trend between the O/P ratio and the chain length n in a log-normal plot gives a slope ranging between 0.24 and 0.30.

4. Discussion

The experimental results clearly indicate that Fischer–Tropsch synthesis over monolithic catalysts is well feasible. First of all, monolithic catalysts could be prepared with different alumina washcoat thicknesses loaded with a Co(Re) active phase. Both the activity and selectivity results of these catalysts are encouraging, considering that the catalytic system is non-optimized and the Co-dispersion is about five times lower than assumed optimal [13], but this can be attributed to an incomplete reduction procedure [14]. Analyzing the results in more detail suggests that in the window studied, diffusion limitations do not play a role for washcoats up to about 50 μm thickness, confirming the work of Hilmen et al. [10], although this does not hold for olefins, see later. Monoliths with thicker washcoats suffer from internal diffusion limitations. These limitations manifest themselves by a lower activity, lower apparent activation energy and higher methane selectivity compared to monoliths with thin washcoat layers. Of these parameters the apparent activation energy changes most, decreasing to about half the value for kinetically controlled process, as expected for diffusion limited processes. The non-systematic trend with the average layer thickness is ascribed to the observed corner rounding and cracks in the layers, especially at thicker coatings (Fig. 2). More cracks in the 110 μm washcoat sample could reduce the effective diffusion distance for the reactants, resulting in a behaviour more resembling the 50 μm sample.

It may seem that diffusion limitations start to a play a role at a rather thin coating of only 50 μm, but it should be reminded that the characteristic diffusion length of a flat coating is its thickness, while in case of, for instance, spherical particles one sixth of the particle diameter is the relevant diffusion distance. Usually particles smaller than 100 μm are suggested to be free from diffusion limitations. With catalyst layers as thin as 50 μm a monolithic reactor with a catalyst volume loading of 25% can be designed [16], similar to that in FTS slurry reactors [17]. The design window up to 50 μm is therefore more than enough for feasible reactor designs. Heat removal, however, has to be performed in harmony with the reactor design. For monoliths the unique situation exists that due to the low pressure drop external heat removal in a liquid loop is feasible [17], like proposed for a highly exothermal dinitrotoluene hydrogenation [18].

Besides a basis for future designs of monolithic catalysts for FTS, this study also provides insight in the nature of secondary reactions and their effects on olefin content and chain growth probability. Iglesia et al. [19] explained non-ASF effects to a combination of secondary reactions of α-olefins and diffusion limitations. The most important parameter in their model is the carbon number dependent diffusivity determining the chances of removal or secondary reaction of reactive products. However, the chain length dependence of the diffusivity needed in their model to fit the experimental results is much stronger than generally found in literature [20]. Kuipers et al. [4] derived an expression for the P/O product ratio, Eq. (1), that includes the effect of solubility and physisorption besides diffusivity to explain non-ASF trends for a flat model catalyst. If diffusion is limiting the relation for the P/O ratio as a function of the chain length n for gas-liquid reaction systems can be expressed as:

$$\frac{P_n}{O_n} \propto \frac{d}{D_n} \exp\left(\frac{n\Delta G_{1\,\mathrm{phys}}}{RT}\right) \propto \exp\left\{(0.2 \pm 0.1)n\right\} n^{0.6} \qquad (1)$$

where $\Delta G_{1\ \mathrm{Phys}}$ represents the incremental increase of Gibbs free energy for physisorption for a CH_2 unit, d the diffusion distance and D_n the diffusivity of a chain of length n. The latter is proportional to $n^{0.6}$. These parameters apply to the olefins since only these react further.

The experimental results of the present study support this model. The slope of the log-normal plot of the O/P ratio versus the chain length parameter n is 0.24–30, well within the estimated range indicated in Eq. (1). This slope represents the increase in Gibbs adsorption energy with increasing chain length. Further, the model predicts an inverse relation between the olefin to paraffin ratio and the diffusion distance. The results of the present study show this relation as well (Fig. 10), but the data are not conclusive enough to determine the relation quantitatively. It suggests, however, that diffusional interference is present with respect to the olefin yield in all results with different monolith layer thicknesses. Kuipers et al. used the paraffin to olefin ratio rather than the non-ASF deviations of the product distributions, as these latter effects are normally too small to be observed experimentally, while the chain length dependence of the P/O ratio is a clearly observable and more

sensitive parameter. This is also clear from the present study, the activity (CO consumption) and methane selectivity change much less than this O/P ratio.

The process of α-olefin readsorption is the same step for both secondary hydrogenation and reinsertion, which makes mechanistic interpretation more difficult. The dominance of secondary hydrogenation compared to reinsertion under certain conditions does not mean that reinsertion is not occurring. Under conditions relatively less favorable for hydrogenation, viz. low temperature and excess carbon monoxide, clear deviation from a single ASF distribution is observed (Fig. 7). The increasing paraffin amounts with chain length (apparent $\alpha > 1$) can only be explained by a model where the olefinic products have (i) a chance to readsorb that exponentially increases with chain length, as in Kuipers' model, and (ii) can be independently hydrogenated, so not reinserted in the chain growth. The reinsertion does not change the ASF distribution, while hydrogenation does. For the total product distribution under these conditions this clearly results in a changing chain propagation parameter α from 0.83 to 0.93. This implies that secondary hydrogenation of olefins is still occurring under these conditions and this phenomenon amplifies with increasing chain length. The lower value for the olefin chain propagation parameter of 0.77 is mainly due to this phenomenon and does not reflect the 'intrinsic' α for these conditions.

The results of this study demonstrate that upon eliminating or minimizing diffusion limitations under the proper operating conditions it is well feasible to produce α-olefins in considerable amounts. A most interesting result was reported recently by Khassin et al. [21]. Using a porous cylindrical catalyst particle in radial flow through mode they observed for the inward flow direction, that compensates for the flow contraction by FTS, only propene as C_3 product. This suggests that olefins may be primary products in FTS, and if they can be removed efficiently in the proper catalyst and reactor configuration they can be obtained as an important product. Together with our results it illustrates the sensitivity of the olefins for consecutive hydrogenation. Nevertheless, FTS may become an interesting route for the production of α-olefins provided olefin/paraffin separation techniques are available.

5. Conclusions

The study shows the feasibility of using monolithic catalysts in Fischer–Tropsch synthesis and yields valuable information about the design parameters for monolithic catalysts in Fischer–Tropsch synthesis. Monoliths with a washcoat layer thicker than about 50 μm suffer from decreased CO conversion activity as a result of diffusion limitations, accompanied by the expected decrease in apparent activation energy. Selectivity to methane also increased, ascribed to increasing H_2/CO ratios deeper inside the layer due to the faster diffusion of hydrogen and a consequently faster hydrogenation of surface species.

The high olefin content of the effluent (O/P ratio), especially for the monoliths with thin washcoats, shows the better accessibility of the catalyst allowing reactive products as α-olefins to escape from the catalyst and may open possibilities to use FTS for production of α-olefins.

The experimental results also offered insight in the secondary reactions affecting the olefin to paraffin ratio and deviations from the ASF product distribution. The chance for olefins to readsorb on the catalyst increases exponentially with increasing chain length, and they are hydrogenated independently of the chain growth process.

Acknowledgement

Corning Inc. is gratefully acknowledgement for supplying the monoliths used in this study.

References

[1] M.F.M. Post, A.C. van't Hoog, J.K. Minderhoud, S.T. Sie, AIChE J. 35 (1989) 1107.
[2] G.P. Van der Laan, A.A.C.M. Beenackers, Catal. Rev. -Sci. Eng. 41 (1999) 255.
[3] E. Iglesia, S.C. Reyes, R.J. Madon, S.L. Soled, Adv. Catal. (1993) 221.
[4] E.W. Kuipers, I.H. Vinkenburg, H. Oosterbeek, J. Catal. 152 (1995) 137.
[5] F. Kapteijn, T.A. Nijhuis, J.J. Heiszwolf, J.A. Moulijn, Catal. Today 66 (2001) 133.
[6] F. Kapteijn, J.J. Heiszwolf, T.A. Nijhuis, J.A. Moulijn, Cattech 3 (1999) 24.
[7] A.F. Pérez-Cadenas, M.M.P. Zieverink, F. Kapteijn, J.A. Moulijn, Catal. Today 105 (2005) 623.
[8] A.M. Hilmen, E. Bergene, O.A. Lindvag, D. Schanke, S. Eri, A. Holmen, Stud. Surf. Sci. Catal. 130 (2000) 1163.
[9] D. Schanke, E. Bergene, A. Holmen, WO/38147 (1998).
[10] A.M. Hilmen, E. Bergene, O.A. Lindvag, D. Schanke, S. Eri, A. Holmen, Catal. Today 69 (2001) 227.
[11] M.C.J. Bradford, M. Te, A. Pollack, Appl. Catal. A: Gen. 283 (2005) 39.
[12] T.A. Nijhuis, A.E.W. Beers, Th. Vergunst, I. Hoek, F. Kapteijn, J.A. Moulijn, Catal. Rev. -Sci. Eng. 43 (2001) 345.
[13] E. Iglesia, Appl. Catal. A: Gen. 161 (1997) 59.
[14] P. Arnoldy, J.A. Moulijn, J. Catal. 93 (1985) 38.
[15] R.M. de Deugd, F. Kapteijn, J.A. Moulijn, Catal. Today 79–80 (2003) 495.
[16] R.M. de Deugd, R.B. Chougule, M.T. Kreutzer, F.M. Meeuse, J. Grievink, F. Kapteijn, J.A. Moulijn, Chem. Eng. Sci. 58 (2003) 583.
[17] R.M. de Deugd, F. Kapteijn, J.A. Moulijn, Top. Catal. 26 (2003) 27.
[18] R.M. Machado, D.J. Parillo, R.P. Boehme, R.R. Broekhuis, US 6005143 (1999).
[19] E. Iglesia, S.C. Reyes, R.J. Madon, J. Catal. 129 (1991) 238.
[20] C. Erkey, J.B. Rodden, A. Akgerman, Energy Fuels 4 (1990) 275.
[21] A.A. Khassin, A.G. Sipatrov, G.K. Chermashetseva, T.M. Yurieva, V.N. Parmon, Top. Catal. 32 (2005) 39.